

## Electronic Supplementary Information

### Effects of Carbon Nanotubes on the Dehydrogenation Behavior of Magnesium Hydride at Relatively Low Temperatures

Wupeng Cai,<sup>\*a</sup> Xiaosong Zhou,<sup>a</sup> Lidong Xia,<sup>a</sup> Kaili Jiang,<sup>b</sup> Shuming Peng,<sup>\*a</sup> Xinggui Long<sup>a</sup> and Jianhua Liang<sup>a</sup>

<sup>a</sup> Institute of Nuclear Physics and Chemistry, China Academy of Engineering Physics, Mianyang 621900, China

<sup>b</sup> Department of Physics and Tsinghua-Foxconn Nanotechnology Research Center, Tsinghua University, Beijing 100084, China

#### S1. Preparation of Powders

Magnesium powder (purity > 99.5 wt%, 300 mesh) and highly purified multi-walled carbon nanotubes (MWCNTs, CNT content > 95 wt%) were purchased and milled in a high energy mill (Simoloyer model CM01-2L, Zoz GmbH) under argon atmosphere with stainless balls (ball-to-powder ratio of 20:1) at a speed of 800 rpm. The weight ratio of MWCNTs is 5 wt%. Some metal particles such as Fe and Ni are still retained in the highly purified MWCNTs, but the total amount of them is below 1.2 wt%. Hence their content in the Mg-CNT composite is so tiny (<0.06 wt%) that their catalytic effect on the sorption kinetics of our samples can be neglected. The sorption kinetics of our samples is much slower than that of the Mg-based composites containing transition-metal catalysts in the previous reports, also indicating the absence of the catalytic effect from transition metals in our samples. Therefore, we can ascribe all the changes of the sorption performance to the effects of CNTs. All the sample handling was done inside a glovebox filled with high-purity argon.

Super-aligned carbon nanotubes (SACNTs) feature strong van der Waals force between tubes.<sup>1,2</sup> Hence a largely expanded (about one hundred times), porous and disordered CNT network can be obtained through ultrasonication in ethanol. Accordingly, the baseline magnesium powder was dispersed in ethanol with 1wt% SACNTs by ultrasonication. SACNTs spread out and Mg particles were uniformly embedded in the SACNT network. Due to the higher density than the solvent, the formed composite fell to the bottom of the container. Then the supernate was removed and the composite was dried at 60 °C for 1 h. Fig. S1 shows the SEM image of the baseline powder after tens of hydriding/dehydriding cycles. Separated MgH<sub>2</sub> particles remained confined in the SACNT network. By contrast, for pure MgH<sub>2</sub> powders without SACNTs, particles were severely sintered to form a nearly whole piece after the treatment at high temperatures. Hence this simple and fast

method is effective to prevent the agglomeration and sintering of  $\text{MgH}_2$  particles and maintain the particle size.

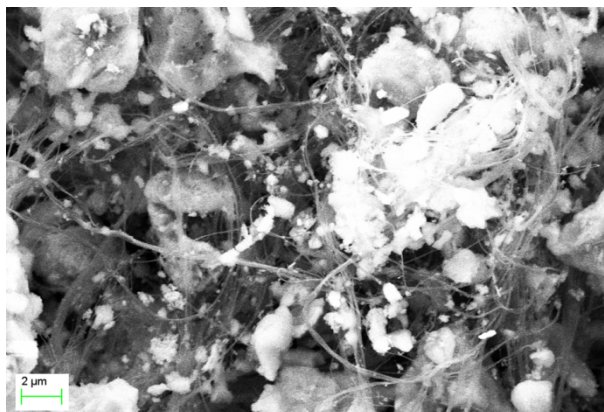


**Fig. S1** SEM image of the baseline powder confined in the network of SACNTs after tens of sorption cycles.

## S2. Methods of Characterization

As-prepared samples were degassed, and then hydrogenated/dehydrogenated for six cycles at 400°C (i.e. activated) using an in-house built automatic Sieverts apparatus. After activated, isothermal desorption kinetics of completely hydrogenated samples were examined in a vacuum at different temperatures. Temperature programmed desorption (TPD) was performed up to 400 °C at 10 K/min in the same apparatus. Scanning electron microscopy (SEM, ZEISS Nvision 40) was utilized to characterize the morphology of samples. Crystal structure was determined using X-ray diffraction (XRD, PANalytical X'pert MRD) with  $\text{Cu K}\alpha$ -radiation, where data were collected from 20° to 110° of  $2\theta$ . Lattice constants and grain size were calculated using a Jade 5.0 program.<sup>3</sup> Lattice dynamics in  $\text{MgH}_2$  and CNT phases were evaluated using Raman spectroscopy (Jobin Yvon LabRAM HR Evolution) with 514.5-nm  $\text{Ar}^+$  laser line (laser power~10 mW) at room temperature.

### S3. Additional Data

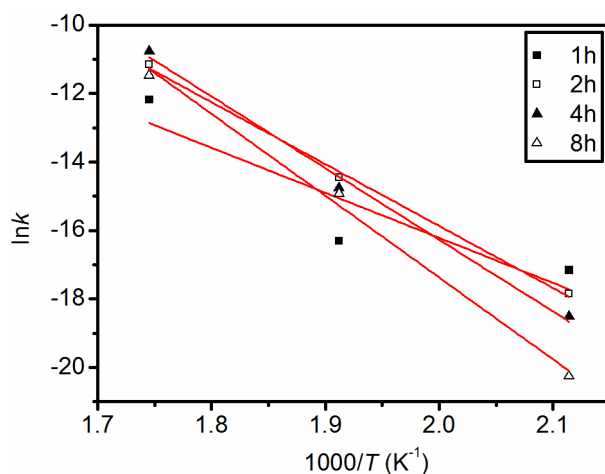


**Fig. S2** Arrhenius plots for the kinetics in the incubation stage of dehydrogenation for MgH<sub>2</sub> from MC1, MC2, MC4 and MC8.

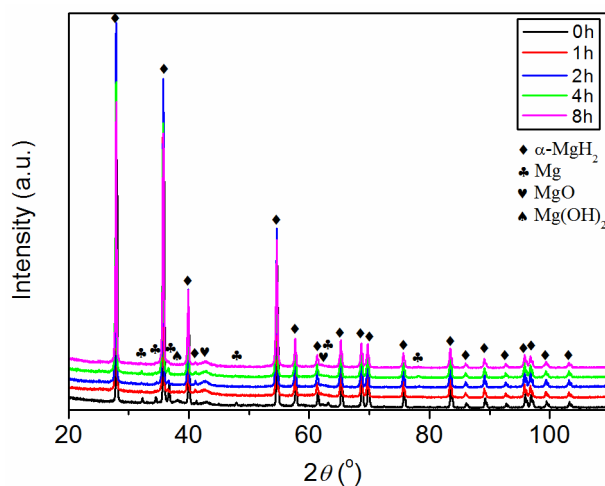


**Fig. S3** XRD spectra of MgH<sub>2</sub> powders from MC0, MC1, MC2, MC4 and MC8. Due to the exposure to air before XRD experiments, small amounts of MgO and Mg(OH)<sub>2</sub> phases are detected.

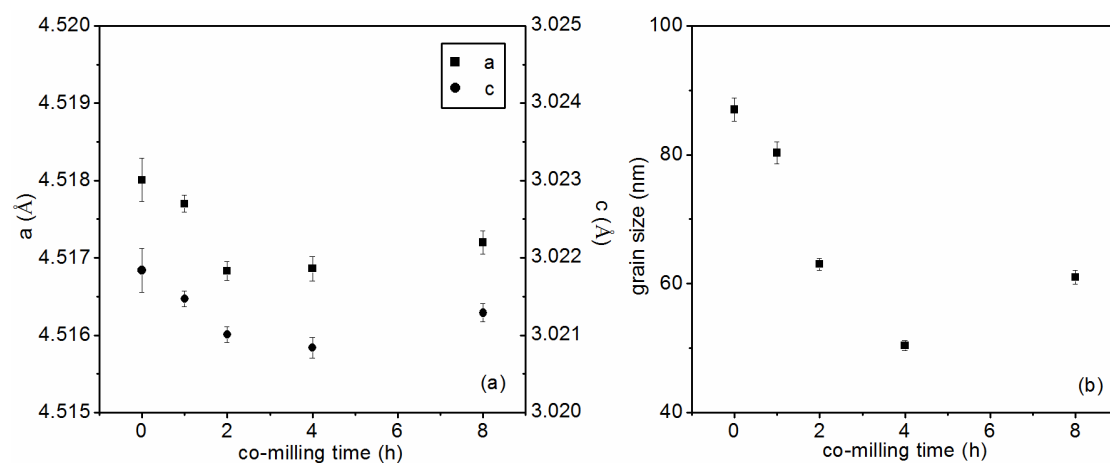


**Fig. S4** Lattice constants (a) and grain size (b) of α-MgH<sub>2</sub> changing with the co-milling time of MWCNTs, calculated from the diffraction peaks in Fig. S3.

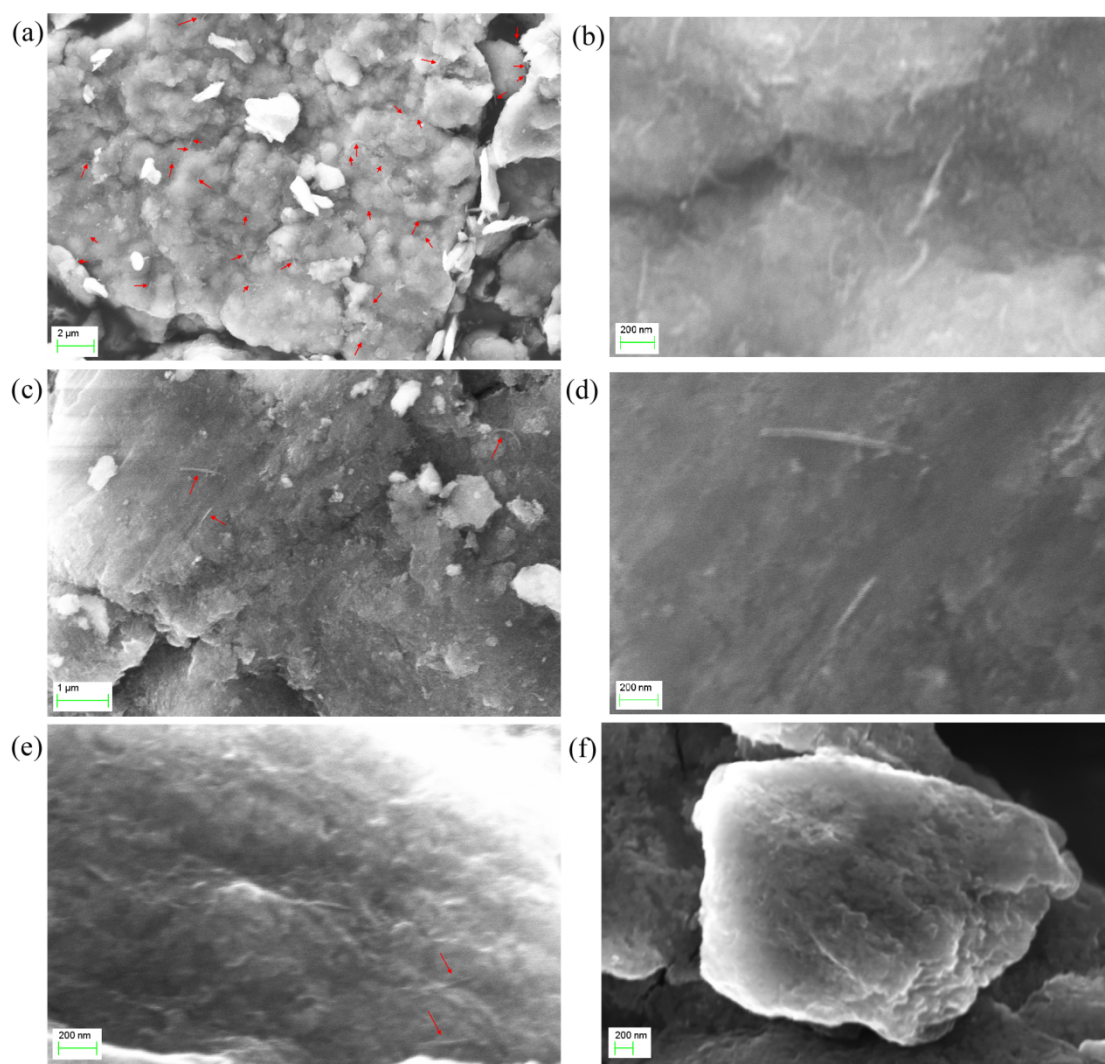


**Fig. S5** SEM observations of CNT segments on the surface of particles in MC1 (a), MC2 (c), MC4 (e) and MC8 (f), indicated by the red arrows. (b) and (d) are the SEM images of MC1 and MC2 at higher magnification, respectively.

#### References:

1. K. L. Jiang, Q. Q. Li and S. S. Fan, *Nature*, 2002, **419**, 801.
2. S. Luo, K. Wang, J. P. Wang, K. L. Jiang, Q. Q. Li and S. S. Fan, *Adv. Mater.*, 2012, **24**, 2294.
3. Jade5.0, XRD Pattern Processing Materials, Data Inc., 1999.